ACS APPLIED MATERIALS & INTERFACES

Research Article

www.acsami.org

Nanostructured Biomaterials from Electrospun Demineralized Bone Matrix: A Survey of Processing and Crosslinking Strategies

Victoria Leszczak,[†] Laura W. Place,[‡] Natalee Franz,[§] Ketul C. Popat,[†,‡] and Matt J. Kipper*[,‡,⊥]

[†]Department of Mechanical Engineering, [‡]School of Biomedical Engineering, [§]Department of Biology, and [⊥]Department of Chemical and Biological Engineering, Colorado State University, 1370 Campus Delivery, Fort Collins, Colorado, United States

ABSTRACT: In the design of scaffolds for tissue engineering biochemical function and nanoscale features are of particular interest. Natural polymers provide a wealth of biochemical function, but do not have the processability of synthetic polymers, limiting their ability to mimic the hierarchy of structures in the natural extracellular matrix. Thus, they are often combined with synthetic carrier polymers to enable processing. Demineralized bone matrix (DBM), a natural polymer, is allograft bone with inorganic material removed. DBM contains the protein components of bone, which includes adhesion ligands and osteoinductive signals, such as important growth factors. Herein we describe a novel method for tuning the nanostructure of DBM through electrospinning without the use of a carrier polymer. This work surveys solvents and solvent blends for electrospinning DBM. Blends of hexafluoroisopropanol and trifluoroacetic acid are studied in detail. The effects of DBM concentration and dissolution time on solution viscosity are also reported and correlated to observed differences in electrospun fiber morphology. We also present a survey of techniques to stabilize the resultant fibers with respect to aqueous environments. Glutaraldehyde vapor treatment is successful at maintaining both macroscopic and microscopic structure of the electrospun DBM fibers. Finally, we report results from tensile testing of stabilized DBM nanofiber mats, and preliminary evaluation of their cytocompatibility. The DBM nanofiber mats exhibit good cytocompatibility toward human dermal fibroblasts (HDF) in a 4-day culture; neither the electrospun solvents nor the cross-linking results in any measurable residual cytotoxicity toward HDF.

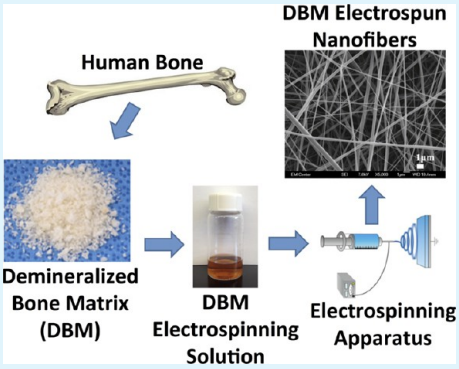

KEYWORDS: *electrospinning, DBM, cross-linking, ECM, nanofibers*

INTRODUCTION

The hierarchy of structures at different length scales is a distinguishing characteristic of all human tissues. These structural features give rise to biological properties that govern tissue function and influence the myriad of processes involved in immune response and tissue repair. In the design of scaffolds for tissue engineering, features at the nanoscale are of particular interest, as cells involved in tissue repair respond to nanoscale topographical features and nanomechanical properties of materials by migrating, differentiating or de-differentiating, and altering their cytokine profiles, and other phenotype indicators.[1−9]

Both synthetic and natural polymers have been researched extensively to create nanoscale scaffolds for engineering various tissues. Synthetic polymers may have tunable degradation kinetics, processability and mechanical properties.[10] However, current scaffolds fabricated from synthetic polymers have surfaces that cells do not recognize unless proteins and peptides are introduced.[11] This lack of recognition may inhibit cell attachment, proliferation and differentiation.[2] Furthermore, synthetic polymers face a challenge when implanted into the body. Despite the fact that they are termed biocompatible and biodegradable, foreign body reactions inhibit the amount of tissue integration, which can ultimately lead to implant failure.[12−15] Natural polymers may be the solution to creating a scaffold that can drive cell proliferation and differentiation, while limiting foreign body reactions.[16,17] Natural polymers such as collagen, glycosaminoglycans, chitosan, and alginates are advantageous because of their low toxicity and low chronic inflammatory response.[18] Unlike synthetic polymers, natural polymers have a complexity that consists of functional peptides, growth factors and bioactive factors which are already present in the body. Therefore, biologically derived materials can possibly provide both a scaffold and a signal for tissue engineering applications, without the addition of growth factors or cytokines.[19] However, many natural polymers do not have the processability of synthetic polymers, limiting their ability to mimic the hierarchy of structures in the natural ECM. Thus, they are often combined with synthetic carrier polymers to facilitate processing into tissue scaffolds.

Demineralized bone matrix (DBM), a natural polymer blend, is allograft bone with inorganic material removed. DBM contains the protein components of bone, including adhesion ligands and osteoinductive signals. It is the natural protein

Received: March 21, 2014
Accepted: May 27, 2014
Published: May 27, 2014

dx.doi.org/10.1021/am501700e | ACS Appl. Mater. Interfaces 2014, 6, 9328−9337

network in which osteocytes perform the anabolic and catabolic processes that maintain healthy bone. Therefore, it can be remodeled and it promotes mineralization. Hence, over the past 30 years, the use of DBM in orthopedic surgery has flourished. However, as prepared, DBM is a dry powder that is typically combined with carrier polymers or other materials to form a composite, paste, or putty that can be more readily used in an orthopedic surgery.[20] Commercial products containing DBM are now available in a variety of different shapes, sizes and forms including morsels, cubes, dowels, strips, etc. However, none of the aforementioned products have tunable nano-features inherent in the osteoconductive nanostructure of bone. Thus, natural polymers such as DBM would be greatly improved for tissue engineering applications if they could be processed into biomimetic nanostructures.

To realize the potential of donated human tissues to develop new tissue constructs, this work establishes techniques to design the nanostructure of DBM. Thus far, DBM products have not been successfully manufactured without the use of a carrier. Further, no DBM products on the market have engineered nanostructured features. Engineering nanostructured materials from human tissues is potentially a simple, low-cost, reproducible strategy for imparting stable biological signals to tissue engineering scaffolds. This strategy may rival or surpass more expensive strategies like growth factor and gene delivery. Herein we describe a novel method for tuning the nanostructure of DBM through electrospinning, a versatile technique for the fabrication of nano-featured surfaces.[21]

To form electrospun nanofibers, a polymer solution is drawn into a fiber by a strong electric field (~kV cm^{-1}) between a nozzle and a grounded collector, while a syringe pump supplies polymer solution to the nozzle. The solvent rapidly evaporates as the polymer solution travels from the nozzle to the collector, resulting in the formation of a nanofiber, collected in a randomly oriented, nonwoven mat. The polymer solution in a volatile solvent must have appropriate surface tension, viscosity, conductivity, and polymer concentration for the process to be successful. Nanofiber scaffolds can be prepared from a wide number of synthetic and natural polymers, providing a three-dimensional cell culture environment, nanoscale topographical and mechanical cues, and a porous network for nutrient and metabolite exchange. Nanofibers from natural polymers have been proposed as tissue engineering scaffolds, including collagen, chitosan, silk, synthetic elastin peptides, and DNA.[22,23] Blends of natural and synthetic polymers (e.g., collagen/polyester and collagen/elastin/polyester) have also been used to make nanofiber scaffolds.[24] Very recently, human adipose tissue ECM has been proposed as a nanofiber scaffold material.[25] To the best of our knowledge, this report from 2012 is the only report in the peer-reviewed literature in which a pure tissue ECM (rather than an ECM component) has been formed into nanofiber tissue scaffolds.

In this work, we survey techniques for production and stabilization of electrospun DBM nanofibers. This novel technique results in a biopolymer construct that is stable in aqueous conditions and contains nanoscale features that recapitulate features of tissue ECM, without the use of a synthetic carrier polymer. Finally, we demonstrate that cross-linked DBM nanofibers are cytocompatible using human dermal fibroblasts.

METHODS

Materials. Morselized demineralized bone matrix (DBM) was generously supplied by Allosource (Centennial, CO). Chloroform, dimethylformamide (DMF), glycerol, methanol, and tetrahydrofuran (THF) were purchased from Mallinckrodt Chemicals (St. Louis, MO). Dichloromethane (DCM), ethanol, hexafluoro-2-propanol (HFIP), and trifluoroacetic acid (TFA), were purchased from Acros Organics (Geel, Belgium). Dimethyl sulfoxide (DMSO) was purchased from EMD Chemicals (Darmstadt, Germany). Acetic acid was purchased from Fisher Scientific (Pittsburgh, PA). Ammonium hydroxide, glutaraldehyde (30 %), riboflavin, and tetrachloroethylene (TCE) were purchased from Sigma-Aldrich (St. Louis, MO). Isopropanol (IPA) was purchased from Macron Chemicals (Phillipsburg, NJ). 1-Ethyl-3-[3-(dimethylamino)propyl]carbodiimide hydrochloride (EDC), HEPES buffer, and tissue culture polystyrene coverslips were purchased from Thermo (Waltham, MA). Phosphate buffered saline (PBS) and trypsin 0.25% were purchased from HyClone (Logan, UT). Antibiotic-antimycotic (anti/anti) was purchased from Gibco (Grand Island, NY). Dulbecco's Modification of Eagle's Medium (DMEM, supplemented with 4.5 g L^{-1} glucose, L-glutamine, and sodium pyruvate) was purchased from Corning Cellgro (Manassas, VA). Fetal bovine serum (FBS) was purchased from Atlanta Biologicals (Flowery Branch, GA). Human dermal fibroblasts (HDF) were purchased from Zen-Bio (Research Triangle Park, NC). LIVE/DEAD Viability/Cytotoxicity Kit for mammalian cells was purchased from Invitrogen (Eugene, OR). CellTiter-Blue cell viability assay was purchased from Promega (Madison, WI). All chemicals were used as received unless indicated otherwise.

Determining Appropriate Solvents for DBM. Solutions were made by adding 0.5 g of DBM to 10 mL of the solvents listed in Table 1 at room temperature (RT) and 65 °C. Solutions of DBM with pure solvents were observed after 18-24 h according to Table 1. Solvent blends were made by combining DMF, DCM, HFIP and glycerol with TFA in 50:50, 70:30 and 90:10 ratios (Table 2). Solutions were made by adding 0.5 g of DBM to these 10 mL solvent blends. Solutions of DBM with solvent blends were observed after 22 h at 40 °C.

Table 1. Dissolution for DBM in Pure Solvents (5 % DBM), at Room Temperature, and at 65 °C

	vapor pressure at 20 °C (Torr)	dielectric constant	soluble at RT	soluble at 65 °C
nonpolar solvents				
chloroform	158.4	4.8	no	no
dichloromethane (DCM)	350	9.1	no	no
polar aprotic solvents				
tetrahydrofuran (THF)	142	7.6	no	no
dimethylformamide (DMF)	2.7	36.7	no	no
dimethyl sulfoxide (DMSO)	<1	46.7	no	no
polar protic solvents				
acetic acid	10.1	6.2	no	partially
trifluoroacetic acid (TFA)	97.5	8.6	**yes**	**yes**
hexafluoroisopropanol (HFIP)	120	16.8	no	partially
glycerol	<1	42.5	no	no
water	17.54	80.1	no	no

Effect of DBM Concentration on Viscosity. To study the effect of DBM concentration on viscosity, solutions of 0.5, 0.8, 1.1, 1.4, 1.7, and 2.0 g of DBM in a 10 mL solvent blend of 70:30 HFIP:TFA were made. Each solution was allowed to dissolve for 22 h at 40 °C. At 22 h, solutions were removed from heat and allowed to reach room

Table 2. Dissolution of DBM in Solvent Blends (5 % DBM at 40 °C for 22 (h)

	50:50	70:30	90:10
DMF:TFA	no	no	no
DCM:TFA	**yes**	**yes**	**yes**
HFIP:TFA	**yes**	**yes**	**yes**
glycerol:TFA	**yes**	**yes**	**yes**

temperature before taking viscosity measurements. Viscosity measurements were taken with a TL5 or TL6 spindle on a Fungilab viscometer attached to a water bath to maintain constant temperature at 25 °C. After taking viscosity measurements, solutions were immediately electrospun at 1 mL h^{-1}, 15 kV and a collector distance of 6 in. Fibers were then coated with a 10 nm layer of gold and imaged at 7 kV on a Jeol JSM-5600F scanning electron microscope (SEM) to examine fiber structure. The images were analyzed using ImageJ, to measure fiber diameters. Between 320 and 450 fiber diameter measurements were obtained from multiple micrographs representing each condition.

Solution Stability. A solution of 1.1 g of DBM in a 10 mL solvent blend of 70:30 HFIP:TFA was made at 40 °C for 22 h. This solution was photographed digitally and then incubated at RT for an additional 48 h. A second photograph was taken at this time and solution color was compared.

This same solution (five different vials for five different time points) was prepared and tested for change in viscosity over time. After 22 h of dissolution, the vials were allowed to cool to RT and the viscosity of the zero time point vial was tested using a TL5 spindle on a Fungilab viscometer attached to a water bath to maintain constant temperature at 25 °C. The other four vials were incubated at RT for 6, 12, 24, or 48 h. At each respective time point, the sample viscosity was measured.

After taking viscosity measurements, each of the solutions was immediately electrospun at 1 mL h^{-1}, 15 kV and a collector distance of 6 in. After spinning, each sample was coated with a 10 nm layer of gold and imaged at 7 kV using an SEM to examine fiber structure. The images were analyzed using ImageJ, to measure fiber diameters. Between 320 and 450 fiber diameter measurements were obtained from multiple micrographs representing each condition.

Stabilizing DBM Fibers. A solution of 1.1 g of DBM in a 10 mL solvent blend of 70:30 HFIP:TFA was made at 40 °C for 22 h and electrospun at 1 mL h^{-1}, 15 kV and a collector distance of 6 in. After spinning, a sample of neat fibers was vacuum dried for 18 h. A number of solvents were investigated for extraction of residual fluorinated solvents from the fibers; these are listed in Table 3. Spot tests were

Table 3. Stability of Fibers in Extractants

extractant	stable
tetrachloroethylene (TCE)	**yes**
chloroform	**yes**
dichloromethane (DCM)	**yes**
hexafluoroisopropanol (HFIP)	no
dimethylformamide (DMF)	no
dimethyl sulfoxide (DMSO)	no
isopropanol (IPA)	**yes**
ethanol	no
methanol	no
aqueous ammonium hydroxide (5 M)	no

done on neat fibers using these solvents to check for solvent compatibility with fibers. TCE was chosen as a likely solvent for the residual TFA and HFIP. Fibers were soaked in TCE for 18 h and dried for analysis. Neat fibers, vacuum dried fibers, TCE-treated fibers, and DBM powder were subjected to X-ray photoelectron spectroscopy (XPS) on a Physical Electronics 5800 spectrometer. Spectra were analyzed using Multipak.

Several cross-linking methods were attempted. Fibers underwent dehydrothermal (DHT) treatment and ultraviolet (UV) light treatment alone and in combination. For DHT treatment, they were placed in a vacuum oven at 150 °C for 18 h. Ultraviolet (UV) treatment was performed at 256 nm for 1 h on each side of the fiber mat. Fibers were then exposed to water to check for stability.

Three covalent chemical cross-linking agents, genipin, 1-ethyl-3-[3-(dimethylamino)propyl] carbodiimide hydrochloride (EDC), and riboflavin were studied. Suitable solvents from Table 3 were chosen for the cross-linking experiments. Suitable solvents in this case are non-solvents for DBM but are able to solubilize the cross-linker. Genipin, at 30 mM, was dissolved in isopropanol (IPA) and fibers were soaked in this solution for 18, 42, or 72 h.[26] A 200 mM solution of EDC in IPA was made and fibers were soaked for 18, 42, or 72 h. EDC-treated fiber mats were rinsed with sodium phosphate buffer (pH 7.4) for 2 h, followed by rinsing with phosphate buffered saline (PBS) for an additional 2 h. This method was adapted from Barnes.[27] This experiment was repeated using dichloromethane (DCM), chloroform, and TCE as solvents for 18 h. Samples of the fiber mats soaked in only the solvent, the solvent + EDC, and the solvent + EDC followed by PBS were then and coated with a 10 nm layer of gold and imaged at 7 kV using SEM.

In situ cross-linking via addition of EDC or riboflavin directly to the spinning solutions was also studied. EDC (38.5 mg mL^{-1}) or riboflavin (2 mg mL^{-1}) was mixed into the electrospinning solution immediately before spinning. The same electrospinning procedure previously described was used here. After electrospinning, the riboflavin sample was exposed to broad spectrum UV light for 1 h. After spinning, fibers were exposed to water to test for stability. Fibers containing riboflavin before and after UV treatment were imaged using SEM.

Finally, cross-linking using glutaraldehyde vapor was investigated. After spinning, fibers supported with aluminum foil were placed into a desiccator with 10 mL of glutaraldehyde (50%). The dessicator was subjected to vacuum for 3 days. After 3 days, fibers were removed and exposed to DI water to remove unreacted glutaraldehyde and to test for stability.[28] Glutaraldehyde-cross-linked fibers before and after exposure to DI water were imaged using SEM.

Mechanical Testing. Uniaxial tensile testing of a dog-bone-shaped sample of glutaraldehyde cross-linked DBM nanofiber mat was performed using a servo-hydraulic mechanical test system (Bionic Model 370.02 MTS Corp, Eden Prairie, MN) equipped with a n 8.9 N load cell (Futek LSB200, Irvine, California). The fiber mat was hydrated with PBS and positioned into customized thin film grips. The fiber mat was speckle coated with India ink and surface images were captured during tensile testing (0.1 % per second with a 0.01 N preload) with a CCD camera (Flea3, Point Grey Research, Richmond, BC, Canada) until mechanical failure occurred.

To calculate strain, images were analyzed using a Matlab (Mathworks, Natick, MA)-based Digital Image Correlation code (E.M.C. Jones, University of Illinois) to track the displacement of the speckle pattern in the central region of each dog-bone-shaped sample. Stress was calculated by dividing the force values by the cross-sectional area of the central region of sample, which had a thickness of 65 μm. Tensile modulus was obtained from the slope of the linear region of the stress-strain curve.

Cytocompatibility Evaluation. DBM samples were soaked in PBS on a shaker plate for 7 days with PBS changes every 24 h, to ensure the complete removal of glutaraldehyde after cross-linking. An 8 mm biopsy punch was used to cut samples of DBM and TCPS for cell culture. These were then treated with ultraviolet light for 1 h for sterilization. HDF were expanded and seeded in DMEM containing 10% FBS, 2.5% HEPES, and 1% anti/anti. HDF were seeded at 100 000 cells/sample (in 200 uL DMEM) in an untreated 48-well plate. Cells were allowed to attach for 3 h, then 300 uL DMEM was added to each well. Samples were moved to a new untreated 48-well plate with fresh DMEM the next day and samples were assayed for cell viability after 24 h of culture. Cell metabolic activity was assayed after 1 day and 4 days of culture, using the CellTiter-Blue assay. Both the viability and metabolic activity of cells on nanofibers were compared to the cells on TCPS.

The Live/Dead assay was used according to manufacturer's instructions. Briefly, three samples of TCPS and three samples of

DBM seeded with HDF and one sample of blank DBM were stained with calcein (2 μM) and ethidium homodimer-1 (4 μM) in PBS for 35 min. Samples were imaged using a Zeiss fluorescence microscope with filter sets 62 HE BP 585/35 (red) and BP 474/28 (green). The CellTiter-Blue cell viability assay was used according to manufacturer's instructions. Briefly, 100 μL of CellTiter-Blue dye was added to 500 μL of DMEM in an untreated 48-well plate containing, three samples of TCPS and three samples of DBM seeded with HDF and three samples of blank TCPS and three samples of blank DBM and incubated for 8 h at 37 °C. Three 150 μL samples were taken from each sample, placed in a black 96-well plate and read in a fluorescence microplate reader (FLUOstar Omega, BMG Labtech, Durham, NC) at 544 nm excitation and 590 nm emission.

RESULTS AND DISCUSSION

Determining Appropriate Solvents for DBM. Prior to electrospinning, an appropriate solvent or solvent blend-capable of dissolving the DBM had to be determined. Initially, pure solvents were used to investigate the solubility of DBM. TFA is the only solvent from Table 1 that can dissolve DBM completely at 5 g dL^{-1} (Table 1) at room temperature and at 65 °C, turning the solution a transparent dark brown color. The dark brown color of the solution may indicate that TFA oxidizes the DBM. TFA is a common electrospinning solvent for synthetic and natural polymers and polymer blends due to its volatility, miscibility with other solvents, and its acidity.[29−33] However, electrospinning the homogenous solution of DBM in TFA at 1 mL h^{-1} was not successful over a range of voltages (0-6 kV) and tip-to-collector distances (5-7in). While attempting to electrospin charge build up and arcing occurred with no fiber formation, limiting the voltage to 6 kV. Therefore, the solution of DBM in TFA does not provide a solution with an ideal viscosity or electrical properties for electrospinning. Thus, blends of solvents with TFA were pursued to increase viscosity and decrease charging, while minimizing oxidation.

Next, solvent blends containing TFA were investigated (Table 2). To potentially preserve the biological function of proteins in DBM, we reduced the dissolution temperature for the solvent blend experiments to 40 °C.[34] DMF:TFA blends do not dissolve DBM; DCM:TFA and glycerol:TFA partially dissolve DBM at 50:50, 70:30, and 90:10 solvent ratios; and HFIP:TFA dissolves DBM at 50:50, 70:30, and 90:10 ratios after 22 h. In addition to not being capable of dissolving the DBM completely, the high volatility of DCM (boiling point = 39.6 °C) hindered its use in preparing the electrospinning solution, and glycerol was too viscous and not volatile enough for use in the electrospinning process. Hence, HFIP was chosen as an appropriate solvent to blend with TFA. By visually inspecting the solutions, it was noted that the 90:10 HFIP:TFA solution was turbid, whereas the 50:50 HFIP:TFA blend was still dark brown in color (Figure 1). Thus, the blend of 70:30 HFIP:TFA was selected, as this composition minimizes the amount of TFA used, while still achieving complete dissolution of the DBM.

Effect of Concentration on Viscosity. The size and uniformity of electrospun fibers is highly dependent on the viscosity of the solution. To reveal how viscosity affects the morphology of DBM fibers, we electrospun various concentrations of DBM (5, 8, 11, 14, 17, and 20 g dL^{-1}) in 70:30 HFIP:TFA. Viscosity of the solutions increased exponentially with solution concentration (Figure 2). Each solution was electrospun and fiber structure was examined with SEM. Representative images and histograms of fiber diameters obtained from multiple images at each condition are shown

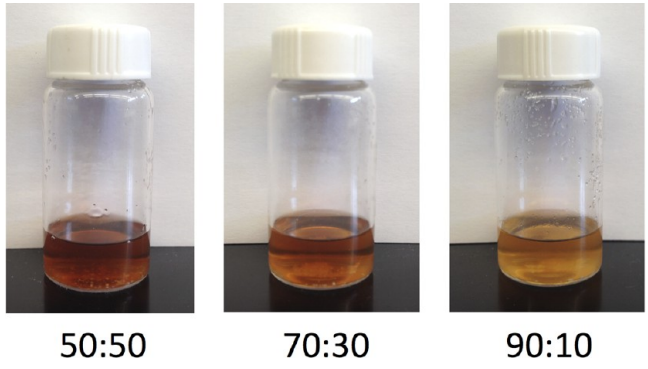

Figure 1. HFIP:TFA blends with 5 % DBM observed after 22 h at 40 °C. The 90:10 HFIP:TFA solution is turbid, whereas the 50:50 HFIP:TFA blend is still dark brown in color. Thus, the 70:30 HFIP:TFA blend was further pursued.

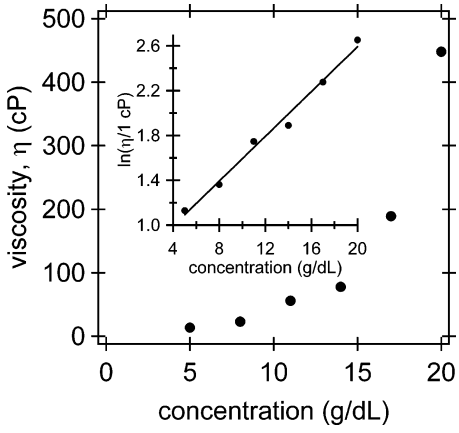

Figure 2. Viscosity of DBM in 70:30 HFIP:TFA increases exponentially with increasing concentration.

in Figure 3. Electrospraying occurred when attempting to electrospin the 5 g dL^{-1} DBM solution (13.5 cP), evident by the presence of particulates in Figure 3A. It is common at low concentrations, when surface tension of the solution is high, for there to be insufficient viscosity and electrical conductivity of the solution, producing beads.[35] As the concentration of DBM and the viscosity of the solution increase, fibers become more uniform and beads disappear. At high polymer concentrations chain entanglements are more readily created, which stabilize the electrospinning jet by inhibiting jet breakup. However, when polymer concentration gets too high, the electrospinning process is also inhibited. This can be seen at 17 g dL^{-1} (189 cP) and 20 g dL^{-1} DBM (448 cP) concentration. At these highest solution concentrations (17 g dL^{-1} and 20 g dL^{-1}) the distribution of fiber diameters becomes non-uniform with some very small fibers (< 100 nm) and some very large fibers (> 1 μm) (Figure 3E, F). This indicates that the appropriate viscosity for electrospinning DBM in a 70:30 HFIP:TFA blend ranges from 23-78 cP. For further experiments the 11 g dL^{-1} DBM concentration (56 cP) was selected.

Solution Stability. To further investigate polymer instability, we took viscosity measurements at 0, 6, 12, 24, and 48 h after dissolution of DBM (11 g dL^{-1} in 70:30 HFIP:TFA). Each of these solutions was then electrospun immediately after viscosity measurements were taken, and fibers were imaged using SEM (Figure 4). Over the first 6 h the viscosity of the solution increases, and then the viscosity decreases over the

dx.doi.org/10.1021/am501700e | ACS Appl. Mater. Interfaces 2014, 6, 9328−9337

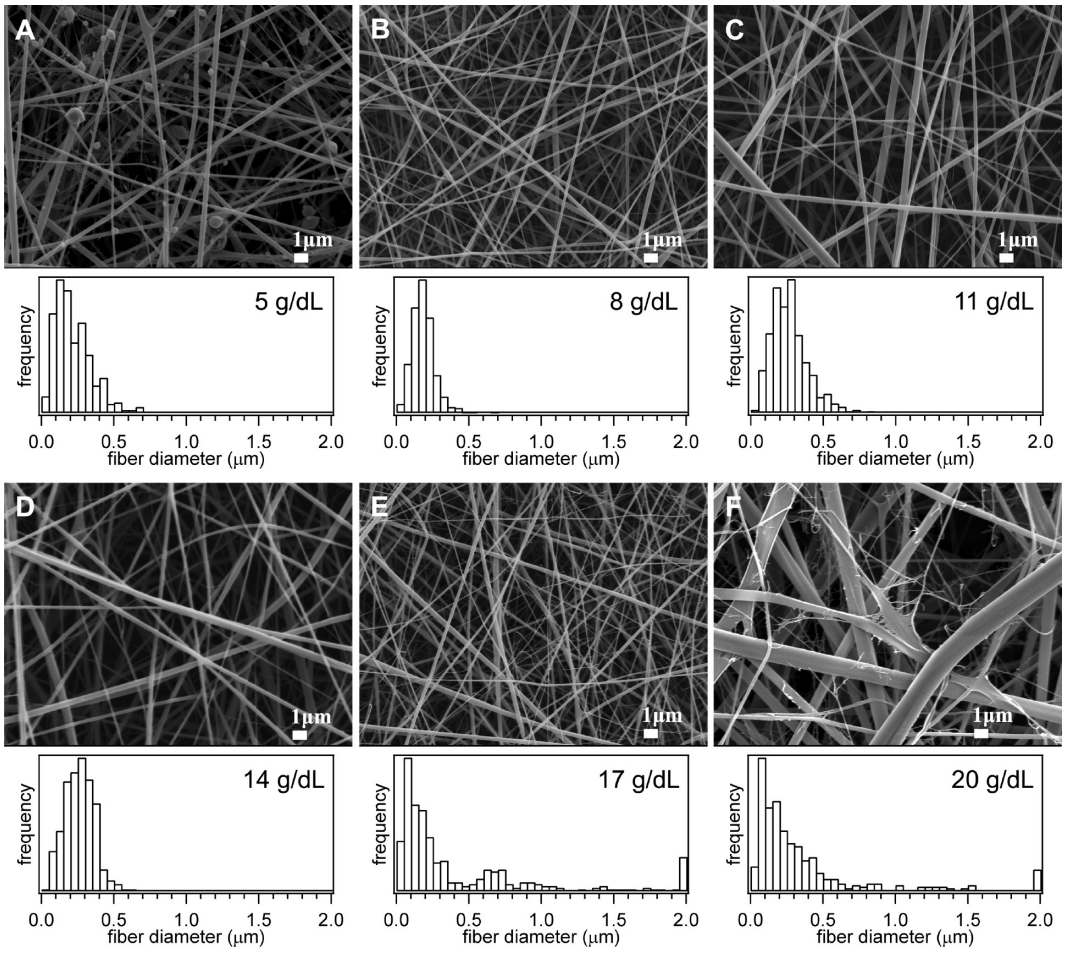

Figure 3. Representative SEM images and fiber diameter distributions reveal that the range of fiber diameter changes with increasing concentrations of DBM. (A) At low DBM concentration (5 g dL^{-1}) the fibers are thinner and beads are present. (B–D) As the concentration increases (8 g dL^{-1} to 14 g dL^{-1}) the fibers become uniform. (E, F) Once the concentration increases to 17 g dL^{-1} however, the fibers are no longer uniform and webbing is observed. In the histograms in E and F, the bars at 2 μm also include all fiber diameters larger than 2 μm.

next 42 h (Figure 4). As previously stated, the polymer solution may be undergoing oxidation, indicating that the polymer is breaking down. Initially, degradation results in a higher concentration of polymer chains, increasing the solution viscosity. This results in the larger diameter fibers and broader fiber diameter distribution observed in Figure 4B. As degradation continues from 6 to 48 h after dissolution, the polymer chains get shorter, and the viscosity then decreases over time, suggesting that fewer entanglements are formed. This results in progressively smaller diameter fibers and narrower fiber diameter distributions as the solution ages (Figures 4C–E). The solution color (not shown), viscosity, and fiber diameter changes over 48 h indicate that the polymer is breaking down over time. This suggests that the solution is unstable and should be used immediately upon preparation.

Stabilizing and Cross-Linking DBM Fibers. After electrospinning from HFIP:TFA solvent blends, the DBM fibers are water-soluble. In order for these to be used as a biomaterial, they must be stable in aqueous environments. X-ray photoelectron spectra (XPS) of electrospun fibers and the neat DBM powder are shown in Figure 5. After electrospinning there is fluorine present that is not present in the DBM powder. This indicates that there is residual solvent remaining in the fibers. Vacuum drying for 18 h was done to remove volatile solvent and XPS was repeated. There was no change in the fluorine peak between neat fibers and vacuum dried fibers. It is possible that the solvent blend used denatured or partially degraded the protein components of the DBM, resulting in a large number of primary amines capable of forming salts with TFA.[29,34,36−39] These salts would make the DBM fibers soluble and cannot be removed by application of vacuum.[29]

To attempt to remove the residual fluorinated solvents, the fibers were exposed to the extractants shown in Table 3 to determine which of these do not solubilize the fibers. These solvents are TCE, chloroform, DCM, and IPA. Of these extractants, TCE was chosen as the most likely to extract the residual solvent. The fibers were exposed to TCE for 18 h and dried. XPS was done on neat fibers and TCE-treated fibers. The fluorine content was reduced by 67 % (XPS data shown in Figure 5), however the fibers were still water-soluble. Thus, cross-linking was explored to stabilize the fibers.

The cross-linking methods explored are summarized in Table 4. DHT and UV treatment were investigated, along with four cross-linking agents, genipin, EDC, riboflavin, and glutaraldehyde. In Table 4, fiber mats that retained mechanical integrity after treatment were determined to be macroscopically stable; fiber mats that also retained the fiber nanostructure observed in SEM were determined to be microscopically stable. DHT alone did not stabilize the fibers, UV treatment and the combination of UV and DHT treatments made the fibers partially insoluble.

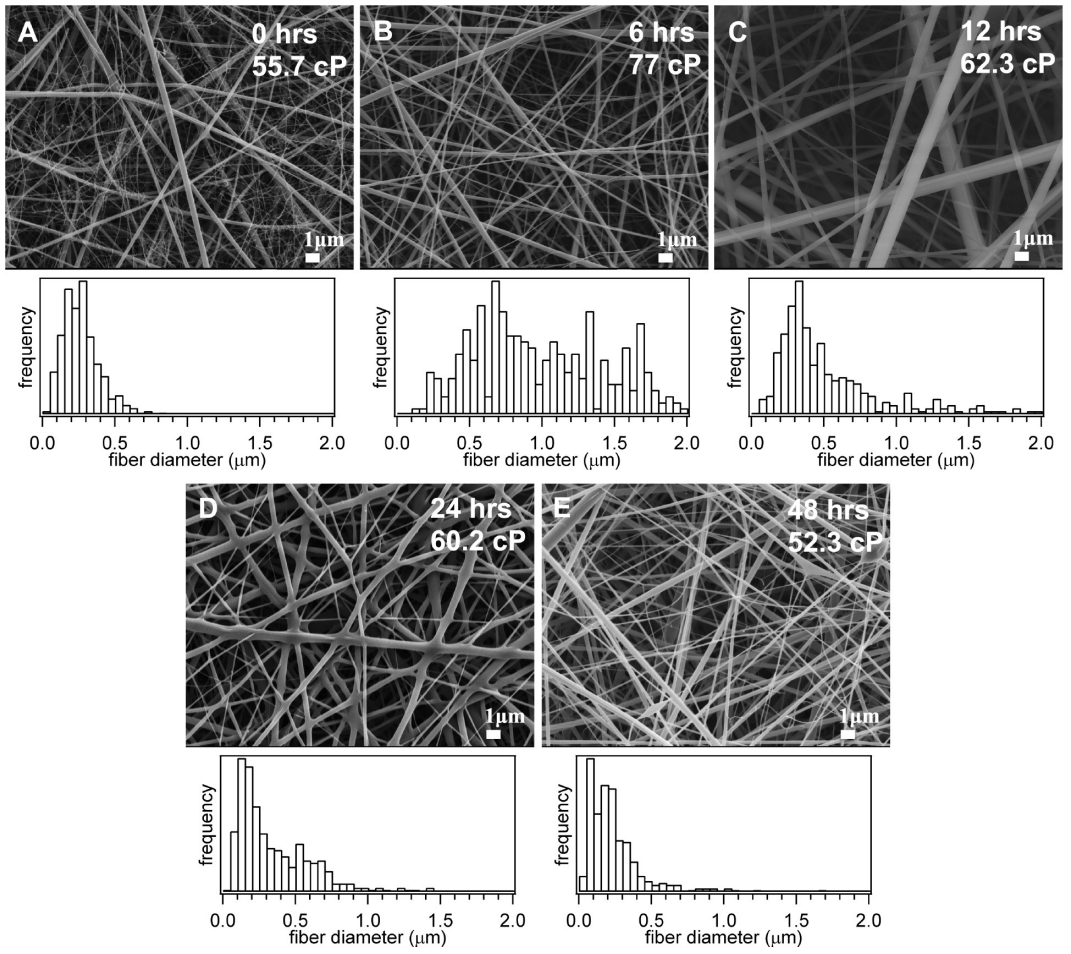

Figure 4. Representative SEM images and fiber diameter distributions of DBM fibers electrospun from solutions (A) immediately after DBM dissolution, (B) 6, (C) 12, (D) 24, and (E) 48 h after dissolution. The higher viscosity solutions (B and C) result in least uniform fiber diameter distribution. As the solution ages and the viscosity goes down, the resulting fiber diameter and distribution width also decrease (D and E).

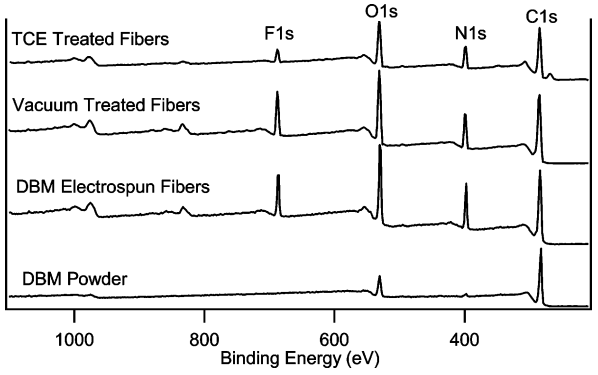

Figure 5. Representative XPS survey scans of DBM powder and electrospun DBM. After electrospinning, a fluorine peak is evident that is not present in the DBM powder. TCE treatment extracts 67 % of the residual fluorinated solvents (TFA and HFIP).

Treatment with DHT cross-links by forming a bond between amine and carboxylate groups through thermal dehydration.[40] Cross-linking via UV treatment is initiated by the formation of free radicals on aromatic rings (e.g., in tyrosine and phenylalanine residues).[41] These free radicals then react with each other to form cross-links. The degree of UV cross-linking is limited by the amount of these structures available. Both DHT and UV treatment may also be limited to the surface of the fibers.[40] When the fibers are exposed to DI water, the water penetrates the fibers causing the mat to dissolve.

Table 4. Stability of Fibers after Different Cross-Linking Protocols

cross-linking conditions	macroscopically stable	microscopically stable
DHT treatment	**yes**	no
UV treatment	partially	no
DHT and UV treatment	partially	no
genipin in IPA	no	no
EDC in chloroform	**yes**	no
EDC in DCM	**yes**	no
EDC in IPA	**yes**	no
EDC in situ	no	no
riboflavin + UV	partially	no
glutaraldehyde vapor	**yes**	**yes**

Chemical treatments were then pursued to more fully cross-link. Genipin is a naturally occurring cross-linking agent derived from the plant *Gardenia jasminoides.*[42] In a study by Sung et al., it was found that genipin is 10 000 times less cytotoxic than glutaraldehyde, making genipin an attractive cross-linking agent for biomaterials. Genipin reacts with free amines found in amino acids and then can dimerize giving rise to both intermolecular and intramolecular bonds.[43] When genipin reacts with amino acids a dark blue pigment is produced.

dx.doi.org/10.1021/am501700e | ACS Appl. Mater. Interfaces 2014, 6, 9328−9337

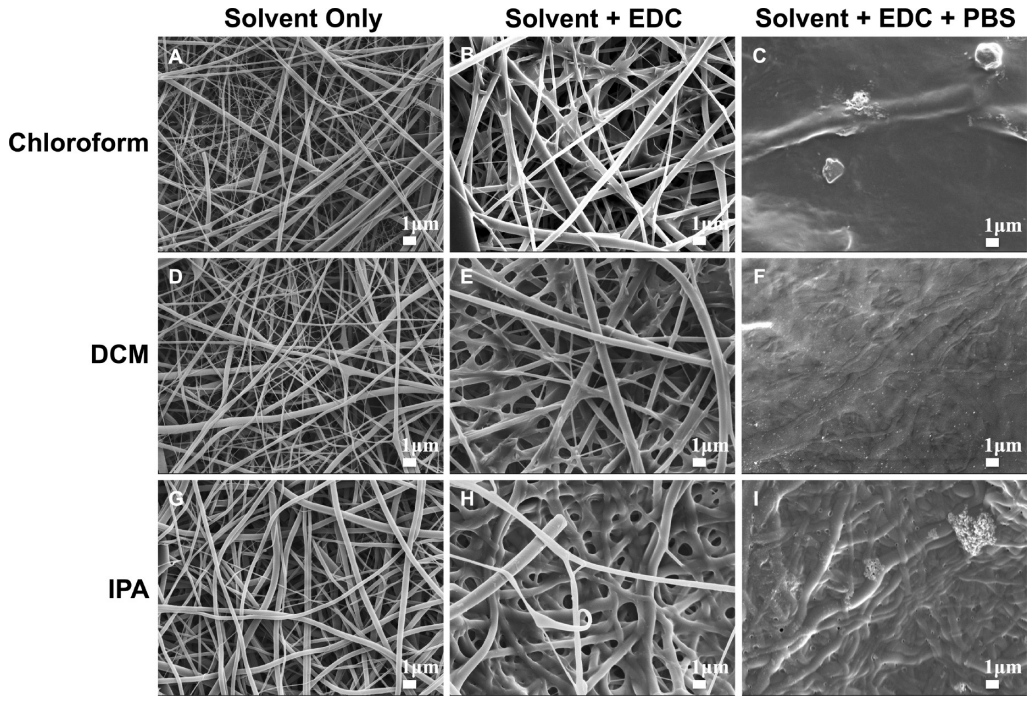

Figure 6. Representative SEM images of the fibers after soaking in (A, D, G) the solvent alone, (B, E, H) the solvent + EDC, and (C, F, I) the solvent + EDC followed by a PBS rinse. Even though cross-linking in chloroform, DCM, and IPA prevents the mats from completely dissolving, in PBS the nanostructure is lost.

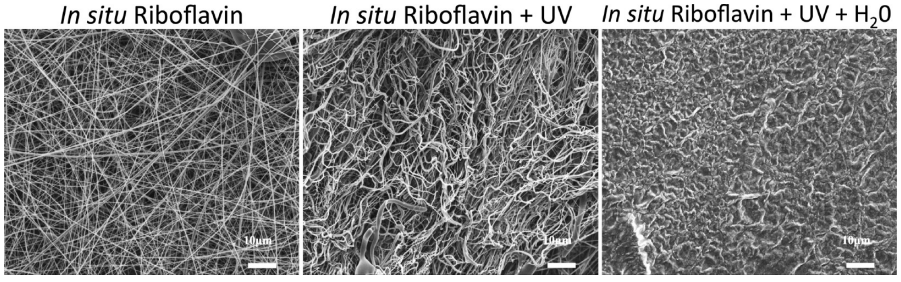

Figure 7. Representative SEM images of the riboflavin-incorporated fibers after electrospinning and after subsequent activation via UV treatment post-spinning. The riboflavin treatment was not able to preserve the nanostructure after exposure to water.

The presence of this pigment is an indication of cross-linking. In this study we dissolved genipin in IPA and soaked fiber mats in the solution for 18−72 h. Dark blue was visible in isolated spots on the fiber mat only after 72 h of treatment, fiber mats treated for shorter periods of time remained white. All genipin-treated fiber mats remained water-soluble after treatment.

EDC forms cross-links between amines and carboxylates. Here, EDC was dissolved in IPA and fiber mats were soaked for 18−72 h. After this treatment fiber mats did not appear water-soluble to the naked eye. The EDC-treated mats were then subjected to a 2-h rinse in phosphate buffer (pH 7.4) followed by a second rinse in phosphate buffered saline (PBS) for an additional 2 h. These were dried and imaged using SEM (Figure 6). After the PBS rinse the fibers are swollen and appear fused. EDC treatment in less polar solvents, DCM, chloroform, and TCE was pursued to minimize fiber swelling. After treatment in DCM and chloroform the mat did not appear to be water-soluble, but EDC was insoluble in TCE and unable to cross-link. Fiber mats were soaked in only the solvent, the solvent + EDC, or solvent + EDC followed by PBS and then imaged using SEM. Representative micrographs are shown in Figure 6. Chloroform + EDC treatment maintains the most fiber structure before the PBS rinse, but all nanostructure is lost after rinsing. The DCM + EDC treatment swells the fibers somewhat, but after rinsing all nanostructure is absent. IPA alone swells the fibers slightly. When EDC is added, a large amount of porosity and some nanostructure is lost. Unlike the less polar solvents, a small amount of the structure is maintained after rinsing with PBS; however, all porosity is eliminated.

A cross-linking agent must be incorporated throughout the fibers in order to successfully stabilize the nanostructure. In nonpolar solvents, the EDC is unable to penetrate inside the fibers to cross-link, and stabilizing bonds are formed only on the outside. When fibers are placed in a polar solvent such as water, the water penetrates the fibers causing them to swell, and cross-links present on the fiber surfaces are insufficient to preserve the nanostructure. IPA is the most polar of these solvents, and thus fibers swell to a greater extent and some EDC is able penetrate inside and form cross-links within, allowing some structure to be maintained.

To achieve more uniform distribution of EDC throughout the fibers, we attempted in situ cross-linking to stabilize the fibers from within. EDC was mixed into the electrospinning

dx.doi.org/10.1021/am501700e | *ACS Appl. Mater. Interfaces* 2014, 6, 9328−9337

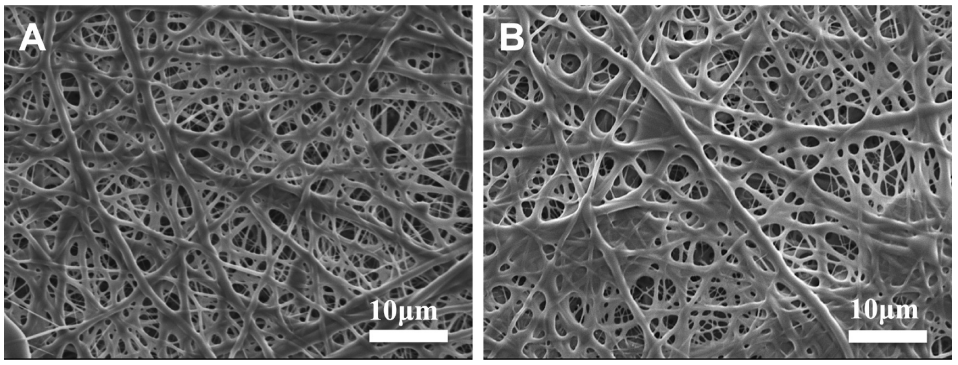

Figure 8. Representative SEM images of glutaraldehyde vapor-treated fibers (A) before and (B) after exposure to water. Glutaraldehyde vapor successfully stabilized the fibers, allowing them to maintain their nanostructure and porosity.

solution immediately before spinning. The same electrospinning procedure previously used was performed. Fibers were exposed to DI water and dissolved immediately. EDC binds amines to carboxylates and TFA contains carboxylates. Therefore, it is possible that the EDC reacted with the TFA instead of with the DBM and no cross-linking occurred within the polymer. A cross-linker that does not react with the solvent is needed. Riboflavin was chosen as a candidate because it cross-links by forming free radicals when exposed to UV light, thus it can be incorporated throughout the fibers and activated when desired.[44] Riboflavin was added to the electrospinning solution, fibers were spun as described earlier, and UV treatment was then performed. The riboflavin incorporation turns the electrospun fibers neon yellow, but after UV exposure the fibers return to a light cream color. SEM images of the riboflavin-containing fibers after electrospinning and after subsequent UV treatment are displayed in Figure 7. The UV-treated fibers exhibit a curled appearance under SEM suggesting that cross-links have been formed within the fibers. However, after UV treatment, these fibers were exposed to DI water and partially dissolved. The two chemical cross-linking agents that react primarily with amines, genipin and riboflavin, do not stabilize fibers; however, EDC treatment (binds amines to carboxylates) resulted in a fiber mat that macroscopically remained intact after contact with water, but lacked fibrous nanostructure.

Unlike the other techniques reviewed above, cross-linking using glutaraldehyde vapor successfully preserves some fiber nanostructure and porosity. Glutaraldehyde creates intra- and intermolecular cross-links by forming an imine with the nonprotonated ϵ-amino group of lysine.[45] After electrospinning, fibers were placed in a dessicator subjected to vacuum with glutaraldehyde for 3 days. Fibers exposed to this treatment were imaged before and after exposure to DI water. While there is significant change to the fiber and pore morphology upon cross-linking, the porous nanostructured network is preserved (Figure 8). Furthermore, the same structure is seen after exposure to DI water, indicating that glutaraldehyde successfully cross-linked the DBM fibers.

Mechanical Testing. Figure 9 shows the stress strain behavior of glutaraldehyde-cross-linked DBM nanofibers after rehydration. The sample exhibits a toe region from about 0% to about 3% strain, followed by a linear elastic region. The ultimate strain of this sample is 8.85% and the Young's modulus obtained from the linear region of the stress–strain curve (between 4% and 8.85% strain) is 3.37 MPa.

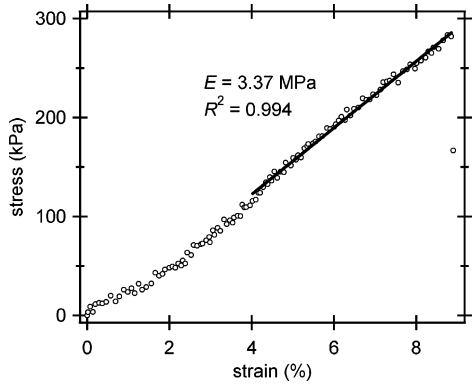

Figure 9. Stress–strain behavior of glutaraldehyde-cross-linked DBM nanofibers under uniaxial tensile testing.

Cytocompatibility Testing. Human dermal fibroblasts (HDF) were cultured on glutaraldehyde-cross-linked DBM nanofibers and on tissue culture polystyrene for 24 h and for 4 days. HDF viability was assayed using Live/Dead staining after 24 h, and metabolic activity was assayed by CellTiter-Blue assay after both 24 h and 4 days. Figure 10 shows a representative merged image of both the green ("live") and red ("dead") channels from fluorescence microscopy of HDF cultured on

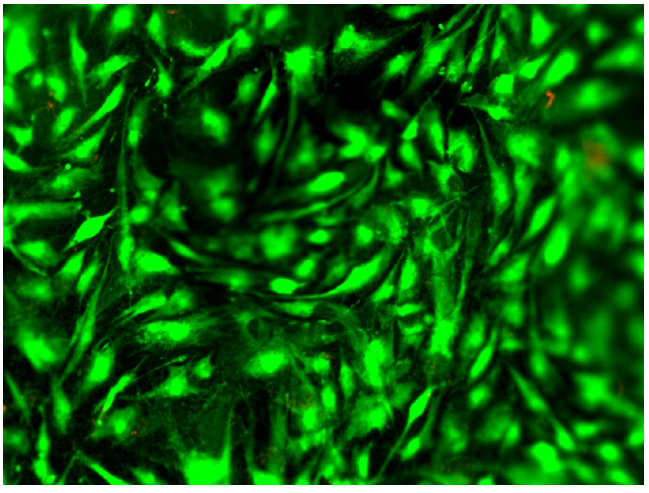

Figure 10. Merged red and green channel fluorescence micrographs of HDF on DBM nanofibers after 24 h of culture. Dead (red) cells could not be quantified, indicating that the DBM nanofibers exhibit good cytocompatibility toward HDF.

dx.doi.org/10.1021/am501700e | ACS Appl. Mater. Interfaces 2014, 6, 9328–9337

DBM nanofibers for 24 h. Dead cells were so sparse, that they could not be meaningfully quantified from multiple fields of view and multiple DBM nanofiber samples, which is similar to the HDF cultured on TCPS (not shown). HDF on nanofibers shown in Figure 10 are well spread and interacting with the fibers. The metabolic activity of HDF cultured on DBM nanofibers was about 40 % lower than that of HDF cultured on TCPS after 24 h (not shown); based on the viability assay, we attribute this apparent reduction in metabolic activity to inefficient cell seeding on the nanofibers rather than to cytotoxicity. After 4 days, there was no change in the metabolic activity on either the HDF cultured on TCPS or HDF cultured DBM nanofibers, indicating good survival of cells on DBM nanofibers. These results confirm that after cross-linking with glutaraldehyde, the DBM nanofibers are stable in aqueous cell culture media, and support mammalian cell growth; neither the solvents used for electrospinning nor the glutaraldehyde cross-linking result in measurable cytotoxicity toward HDF. Furthermore, the HDF on DBM nanofibers are well-spread, indicating that DBM nanofibers require no exogenous adhesion ligand modification (e.g., addition of fibronectin, collagen, or RGD peptides) as are commonly required to promote cell adhesion to many synthetic polymer scaffolds.

CONCLUSIONS

DBM is completely soluble in TFA, but the solution does not exhibit properties conducive to electrospinning. After exploring a number of solvent blends, we chose 70:30 HFIP:TFA as having ideal properties for electrospinning. DBM concentration in the spinning solution affects fiber morphology because of changes in viscosity and polymer entanglements. Electrospraying is observed at low concentrations, uniform fibers are observed at intermediate concentrations, and fiber diameter becomes widely variable at high concentrations. DBM is being degraded by the solvent mixture over time. This degradation affects solution viscosity, fiber morphology, and stability of fibers in aqueous environments. Initially, viscosity and fiber diameter increase because of a higher number of polymer chains in solution, but as degradation continues and polymer chains become shorter, viscosity and fiber diameter decrease. In order to have consistent fiber mats solutions may not be stored for later use. After the electrospinning process, the fiber mats are water-soluble. Crosslinking is imperative for the success of using DBM as electrospun tissue engineering scaffolds. Thus, far, the only cross-linking method that is capable of maintaining fiber structure and porosity is a glutaraldehyde vapor treatment. After glutaraldehyde cross-linking, rehydrated DBM nanofibers have good handling characteristics, and are stable in aqueous environments. Importantly, initial cytocompatibility testing gives no indication of cytotoxicity that might be caused by electrospinning solvents or residual glutaraldehyde, and the DBM nanofibers support cell attachment with no addition of exogenous adhesion ligands.

AUTHOR INFORMATION

Corresponding Author

*E-mail: matthew.kipper@colostate.edu. Tel.: +970 491 0870. Fax: +1 970 491 7369.

Author Contributions

V.L. and L.W.P. contributed equally to this work. The manuscript was written through contributions of all authors. All authors have given approval to the final version of the manuscript.

Funding

Funding for this work was provided by Allosource.

Notes

The authors declare no competing financial interest.

ACKNOWLEDGMENTS

We thank Brent Atkinson for helpful discussions regarding applications and formulations of DBM. We thank Prof. Tammy Haut Donahue and Hannah Pauly for use of the mechanical testing apparatus.

ABBREVIATIONS

DBM, demineralized bone matrix
TFA, trifluoroacetic acid
HFIP, hexafluoroisopropanol
DCM, dichloromethane
IPA, isopropanol
THF, tetrahydrofuran
DMF, dimethylformamide
DMSO, dimethyl sulfoxide
TCE, tetrachloroethylene
DHT, dehydrothermal treatment
UV, ultraviolet
EDC, 1-ethyl-3-[3-(dimethylamino)propyl]carbodiimide hydrochloride

REFERENCES

(1) Mendonça, G.; Mendonça, D. B. S.; Simões, L. G. P.; Araújo, A. L.; Leite, E. R.; Duarte, W. R.; Aragão, F. J. L.; Cooper, L. F. The Effects of Implant Surface Nanoscale Features on Osteoblast-Specific Gene Expression. *Biomaterials* **2009**, *30*, 4053−4062.

(2) Yim, E. K. F.; Pang, S. W.; Leong, K. W. Synthetic Nanostructures Inducing Differentiation of Human Mesenchymal Stem Cells into Neuronal Lineage. *Exp. Cell Res.* **2007**, *313*, 1820−1829.

(3) Gittens, R. A.; McLachlan, T.; Olivares-Navarrete, R.; Cai, Y.; Berner, S.; Tannenbaum, R.; Schwartz, Z.; Sandhage, K. H.; Boyan, B. D. The Effects of Combined Micron-/Submicron-Scale Surface Roughness and Nanoscale Features on Cell Proliferation and Differentiation. *Biomaterials* **2011**, *32*, 3395−3403.

(4) Andersson, A.-S.; Bäckhed, F.; von Euler, A.; Richter-Dahlfors, A.; Sutherland, D.; Kasemo, B. Nanoscale Features Influence Epithelial Cell Morphology and Cytokine Production. *Biomaterials* **2003**, *24*, 3427−3436.

(5) Popat, K. C.; Eltgroth, M.; LaTempa, T. J.; Grimes, C. A.; Desai, T. A. Titania Nanotubes: A Novel Platform for Drug-Eluting Coatings for Medical Implants? *Small* **2007**, *3*, 1878−1881.

(6) Cui, F.-Z.; Ge, J. New Observations of the Hierarchical Structure of Human Enamel, from Nanoscale to Microscale. *J. Tissue Eng. Regener. Med.* **2007**, *1*, 185−191.

(7) Wang, X.; Kim, H. J.; Wong, C.; Vepari, C.; Matsumoto, A.; Kaplan, D. L. Fibrous Proteins and Tissue Engineering. *Mater. Today* **2006**, *9*, 44−53.

(8) Boddohi, S.; Kipper, M. J. Engineering Nanoassemblies of Polysaccharides. *Adv. Mater.* **2010**, *22*, 2298−3016.

(9) Ruckh, T. T.; Kumar, K.; Kipper, M. J.; Popat, K. C. Osteogenic Differentiation of Bone Marrow Stromal Cells on Poly([Epsilon]-Caprolactone) Nanofiber Scaffolds. *Acta Biomater.* **2010**, *6*, 2949−2959.

(10) Gunatillake, P. A.; Adhikari, R. Biodegradable Synthetic Polymers for Tissue Engineering. *Eur. Cells Mater.* **2003**, *5*, 1−16.

(11) Henderson, L. A.; Kipper, M. J.; Chiang, M. Y. M. In *Polymers for Biomedical Applications*; Mahapatro, A., Kulshrestha, A. S., Eds.;

American Chemical Society: Washington, D.C., 2008; Chapter 8, pp 118−152.
(12) Marotta, J. S.; Widenhouse, C. W.; Habal, M. B.; Goldberg, E. P. Silicone Gel Breast Implant Failure and Frequency of Additional Surgeries: Analysis of 35 Studies Reporting Examination of More Than 8000 Explants. *J. Biomed. Mater. Res.* **1999**, *48*, 354−364.
(13) Tullberg, T. Failure of a Carbon Fiber Implant: A Case Report. *Spine* **1998**, *23*, 1804−1806.
(14) van der Giessen, W. J.; Lincoff, A. M.; Schwartz, R. S.; van Beusekom, H. M. M.; Serruys, P. W.; Holmes, D. R.; Ellis, S. G.; Topol, E. J. Marked Inflammatory Sequelae to Implantation of Biodegradable and Nonbiodegradable Polymers in Porcine Coronary Arteries. *Circulation* **1996**, *94*, 1690−1697.
(15) Leszczak, V.; Smith, B. S.; Popat, K. C. Hemocompatibility of Polymeric Nanostructured Surfaces. *J. Biomater. Sci.-Polym. Ed.* **2013**, *24*, 1529−1548.
(16) Furst, E. M.; Pagac, E. S.; Tilton, R. D. Coadsorption of Polylysine and the Cationic Surfactant Cetyltrimethylammonium Bromide on Silica. *Ind. Eng. Chem. Res.* **1996**, *35*, 1566−1574.
(17) Becker, T. A.; Kipke, D. R.; Brandon, T. Calcium Alginate Gel: A Biocompatible and Mechanically Stable Polymer for Endovascular Embolization. *J. Biomed. Mater. Res.* **2001**, *54*, 76−86.
(18) Vats, A.; Tolley, N. S.; Polak, J. M.; Gough, J. E. Scaffolds and Biomaterials for Tissue Engineering: A Review of Clinical Applications. *Clin. Otolaryngol. Allied Sci.* **2003**, *28*, 165−172.
(19) Renth, A. N.; Detamore, M. S. Leveraging "Raw Materials" as Building Blocks and Bioactive Signals in Regenerative Medicine. *Tissue Eng., Part B* **2012**, *18*, 341−62.
(20) Gruskin, E.; Doll, B. A.; Futrell, F. W.; Schmitz, J. P.; Hollinger, J. O. Demineralized Bone Matrix in Bone Repair: History and Use. *Adv. Drug Delivery Rev.* **2012**, *64*, 1063−1077.
(21) Murugan, R.; Ramakrishna, S. Nano-Featured Scaffolds for Tissue Engineering: A Review of Spinning Methodologies. *Tissue Eng.* **2006**, *12*, 435−447.
(22) Holzwarth, J. M.; Ma, P. X. Biomimetic Nanofibrous Scaffolds for Bone Tissue Engineering. *Biomaterials* **2011**, *32*, 9622−9629.
(23) Pham, Q. P.; Sharma, U.; Mikos, A. G. Electrospinning of Polymeric Nanofibers for Tissue Engineering Applications: A Review. *Tissue Eng.* **2006**, *12*, 1197−1211.
(24) Heydarkhan-Hagvall, S.; Schenke-Layland, K.; Dhanasopon, A. P.; Rofail, F.; Smith, H.; Wu, B. M.; Shemin, R.; Beygui, R. E.; MacLellan, W. R. Three-Dimensional Electrospun ECM-Based Hybrid Scaffolds for Cardiovascular Tissue Engineering. *Biomaterials* **2008**, *29*, 2907−2914.
(25) Francis, M. P.; Sachs, P. C.; Madurantakam, P. A.; Sell, S. A.; Elmore, L. W.; Bowlin, G. L.; Holt, S. E. Electrospinning Adipose Tissue-Derived Extracellular Matrix for Adipose Stem Cell Culture. *J. Biomed. Mater. Res., Part A* **2012**, *100A*, 1716−1724.
(26) Yao, C. H.; Liu, B. S.; Chang, C. J.; Hsu, S. H.; Chen, Y. S. Preparation of Networks of Gelatin and Genipin as Degradable Biomaterials. *Mater. Chem. Phys.* **2004**, *83*, 204−208.
(27) Barnes, C. P.; Pemble, C. W.; Brand, D. D.; Simpson, D. G.; Bowlin, G. L. Cross-Linking Electrospun Type II Collagen Tissue Engineering Scaffolds with Carbodiimide in Ethanol. *Tissue Eng.* **2007**, *13*, 1593−605.
(28) Zhang, Y. Z.; Venugopal, J.; Huang, Z. M.; Lim, C. T.; Ramakrishna, S. Crosslinking of the Electrospun Gelatin Nanofibers. *Polymer* **2006**, *47*, 2911−2917.
(29) Almodóvar, J.; Kipper, M. J. Coating Electrospun Chitosan Nanofibers with Polyelectrolyte Multilayers Using the Polysaccharides Heparin and N,N,N-Trimethyl Chitosan. *Macromol. Biosci.* **2011**, *11*, 72−76.
(30) Devarayan, K.; Hanaoka, H.; Hachisu, M.; Araki, J.; Ohguchi, M.; Behera, B. K.; Ohkawa, K. Direct Electrospinning of Cellulose-Chitosan Composite Nanofiber. *Macromol. Mater. Eng.* **2013**, *298*, 1059−1064.
(31) Ohkawa, K.; Cha, D. I.; Kim, H.; Nishida, A.; Yamamoto, H. Electrospinning of Chitosan. *Macromol. Rapid Commun.* **2004**, *25*, 1600−1605.
(32) Ohsawa, O.; Lee, K. H.; Kim, B. S.; Lee, S.; Kim, I. S. Preparation and Characterization of Polyketone (PK) Fibrous Membrane Via Electrospinning. *Polymer* **2010**, *51*, 2007−2012.
(33) Chen, F.; Li, X. Q.; Mo, X. M.; He, C. L.; Wang, H. S.; Ikada, Y. Electrospun Chitosan-P(LLA-Cl) Nanofibers for Biomimetic Extracellular Matrix. *J. Biomater. Sci., Polym. Ed.* **2008**, *19*, 677−691.
(34) Côté, M.-F.; Laroche, G.; Gagnon, E.; Chevallier, P.; Doillon, C. J. Denatured Collagen as Support for a FGF-2 Delivery System: Physicochemical Characterizations and in Vitro Release Kinetics and Bioactivity. *Biomaterials* **2004**, *25*, 3761−3772.
(35) Zheng, J.; He, A.; Li, J.; Xu, J.; Han, C. C. Studies on the Controlled Morphology and Wettability of Polystyrene Surfaces by Electrospinning or Electrospraying. *Polymer* **2006**, *47*, 7095−7102.
(36) Sangsanoh, P.; Supaphol, P. Stability Improvement of Electrospun Chitosan Nanofibrous Membranes in Neutral or Weak Basic Aqueous Solutions. *Biomacromolecules* **2006**, *7*, 2710−2714.
(37) Jiang, Q. R.; Reddy, N.; Zhang, S. M.; Roscioli, N.; Yang, Y. Q. Water-Stable Electrospun Collagen Fibers from a Non-Toxic Solvent and Crosslinking System. *J. Biomed. Mater. Res., Part A* **2013**, *101A*, 1237−1247.
(38) Arnoult, O. A Novel Benign Solution for Collagen Processing. *PhD Thesis*, Case Western Reserve University, Cleveland, OH, 2010.
(39) Chen, Z. G.; Wang, P. W.; Wei, B.; Mo, X. M.; Cui, F. Z. Electrospun Collagen−Chitosan Nanofiber: A Biomimetic Extracellular Matrix for Endothelial Cell and Smooth Muscle Cell. *Acta Biomater.* **2010**, *6*, 372−382.
(40) Ratanavaraporn, J.; Rangkupan, R.; Jeeratawatchai, H.; Kanokpanont, S.; Damrongsakkul, S. Influences of Physical and Chemical Crosslinking Techniques on Electrospun Type A and B Gelatin Fiber Mats. *Int. J. Biol. Macromol.* **2010**, *47*, 431−438.
(41) Weadock, K. S.; Miller, E. J.; Bellincampi, L. D.; Zawadsky, J. P.; Dunn, M. G. Physical Cross-Linking of Collagen-Fibers - Comparison of Ultraviolet-Irradiation and Dehydrothermal Treatment. *J. Biomed. Mater. Res.* **1995**, *29*, 1373−1379.
(42) Muzzarelli, R. A. A. Genipin-Crosslinked Chitosan Hydrogels as Biomedical and Pharmaceutical Aids. *Carbohydr. Polym.* **2009**, *77*, 1−9.
(43) Sung, H. W.; Chen, C. N.; Huang, R. N.; Hsu, J. C.; Chang, W. H. In Vitro Surface Characterization of a Biological Patch Fixed with a Naturally Occurring Crosslinking Agent. *Biomaterials* **2000**, *21*, 1353−1362.
(44) Fawzy, A.; Nitisusanta, L.; Iqbal, K.; Daood, U.; Beng, L. T.; Neo, J. Characterization of Riboflavin-Modified Dentin Collagen Matrix. *J. Dent. Res.* **2012**, *91*, 1049−1054.
(45) Gough, J. E.; Scotchford, C. A.; Downes, S. Cytotoxicity of Glutaraldehyde Crosslinked Collagen/Poly(Vinyl Alcohol) Films Is by the Mechanism of Apoptosis. *J. Biomed. Mater. Res.* **2002**, *61*, 121−130.